

# Chapter 2

## Thyroid Ultrasound Physics

**Robert A. Levine**

### Abbreviations

Hz	Hertz
MHz	Megahertz
m/s	Meters per second

### Sound and Sound Waves

Some animal species such as dolphins, whales, and bats are capable of creating a “visual” image based on receiving reflected sound waves. Our unassisted vision is limited to electromagnetic waves in the spectrum of visible light. Humans require technology and an understanding of physics to use sound to create a picture. This chapter will explore how we have developed a technique for creating a visual image from sound waves [1].

---

R.A. Levine, MD, FACE, ECNU  
Geisel School of Medicine at Dartmouth College, Thyroid Center  
of New Hampshire, St. Joseph Hospital, Nashua, NH, USA  
e-mail: [thyroidmd2@gmail.com](mailto:thyroidmd2@gmail.com)

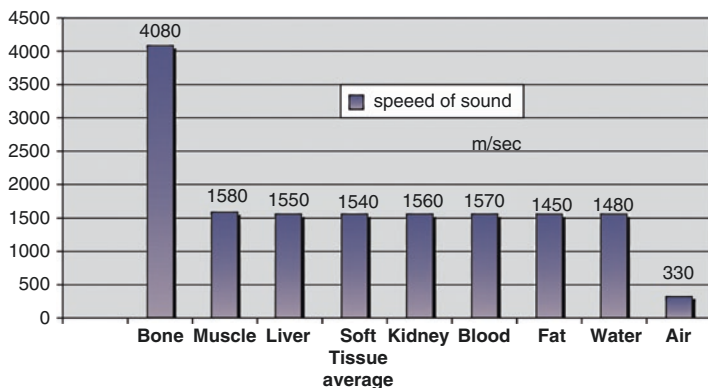


FIGURE. 2.1 Speed of sound. The speed of sound is constant for a specific material and does not vary with frequency. Speed of sound for various biological tissues is illustrated

Sound is transmitted as mechanical energy, in contrast to light, which is transmitted as electromagnetic energy. Unlike electromagnetic waves, sound waves require a propagating medium. Light is capable of traveling through a vacuum, but sound will not transmit through a vacuum. The qualities of the transmitting medium have a direct effect on how sound is propagated. Materials have different speeds of sound transmission and acoustic impedance. Speed of sound is constant for a specific material and does not vary with sound frequency (Fig. 2.1). Acoustic impedance is a measure of the opposition that a system presents to the flow of acoustic energy. When sound travels through a material and encounters a boundary separating two different areas of acoustic impedance, a portion of the sound energy will be reflected, and the remainder will be transmitted. The amount reflected is proportionate to the degree of mismatch of acoustic impedance. Acoustic impedance of a material depends on its density, stiffness, and speed of sound [2].

Sound waves propagate by compression and rarefaction of molecules in space (Fig. 2.2). Molecules of the propagating

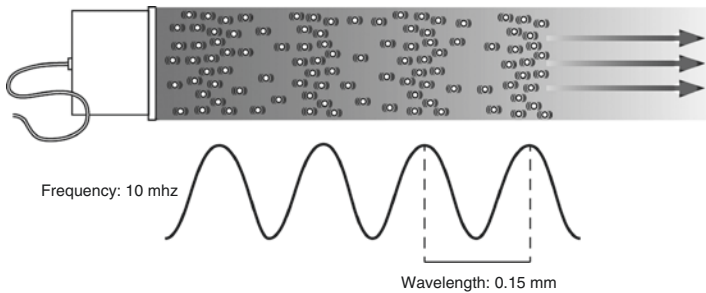


FIGURE. 2.2 Sound waves propagate in a longitudinal direction but are typically represented by a sine wave where the peak corresponds to the maximum compression of molecules in space, and the trough corresponds to the maximum rarefaction

medium vibrate around their resting position and transfer their energy to neighboring molecules. Sound waves carry energy rather than matter through space.

As shown in Fig. 2.2, sound waves propagate in a longitudinal direction but are typically represented graphically by a sine wave where the peak corresponds to the maximum compression of molecules in space, and the trough corresponds to the maximum rarefaction. Frequency is defined as the number of cycles per time of the vibration of the sound waves. A Hertz (Hz) is defined as one cycle per second. The audible spectrum is between 30 and 20,000 Hz. Ultrasound is defined as sound waves at a higher frequency than the audible spectrum. Typical frequencies used in diagnostic ultrasound vary between five million and sixteen million cycles per second (5 and 16 MHz) [1, 3].

Diagnostic ultrasound uses pulsed waves, allowing for an interval of sound transmission, followed by an interval during which reflected sounds are received and analyzed. Typically three cycles of sound are transmitted as a pulse. The spatial pulse length is the length in space filled by three cycles (Fig. 2.3). Spatial pulse length is one of the determinants of resolution. Since higher frequencies have a smaller pulse

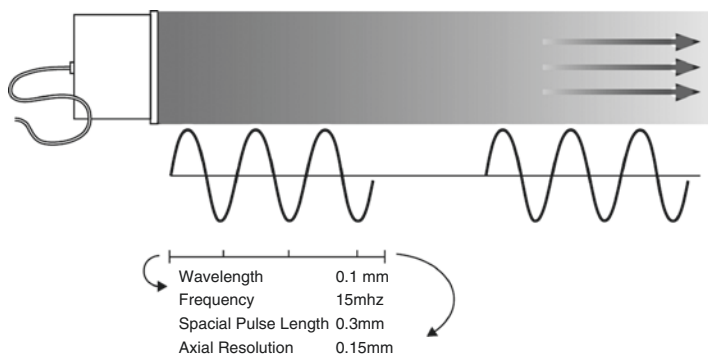


FIGURE. 2.3 Diagnostic ultrasound uses pulsed waves, allowing for an interval of sound transmission, followed by an interval during which reflected sounds are received and analyzed. Typically three cycles of sound are transmitted as a pulse

length, higher frequencies are associated with improved resolution. As illustrated in Fig. 2.3, at a frequency of 15 MHz, the wavelength in biological tissues is approximately 0.1 mm, allowing an axial resolution of 0.15 mm. Although resolution improves with increased frequency, the depth of penetration of the ultrasound waves decreases, limiting the visualization of deeper structures.

As mentioned above, the *speed of sound* is constant for a given material or biological tissue. It is not affected by frequency or wavelength. It increases with stiffness and decreases with density of the material. As seen in Fig. 2.1, common biologic tissues have different propagation velocities. Bone, as a very dense and stiff tissue, has a high propagation velocity of 4080 meters per second (m/s). Fat tissue, with low stiffness and low density, has a relatively low speed of sound of 1450 m/s. Most soft tissues have a speed of sound near 1540 m/s. Muscle, liver, and thyroid have a slightly faster speed of sound. By convention, all ultrasound equipment uses an average speed of 1540 m/s. The distance

to an object displayed on an ultrasound image is calculated by multiplying the speed of sound by half of the time interval for a sound signal to return to the transducer [2, 3]. By using the accepted 1540 m/s as the assumed speed of sound, all ultrasound equipment will provide identical distance or size measurements.

*Reflection* is the redirection of a portion of a sound wave from the interface of tissues with unequal acoustic impedance. Larger differences in impedance will result in greater amounts of reflection. A material that is homogeneous in acoustic impedance does not generate any internal echoes. A pure cyst is a typical example of an anechoic (echoless) structure. Most biological tissues have varying degrees of inhomogeneity both on a cellular and macroscopic level. Connective tissue, blood vessels, and cellular structure all provide mismatches of acoustic impedance, which lead to the generation of characteristic ultrasonographic patterns (Figs. 2.4, 2.5, and 2.6).



FIGURE. 2.4 The echotexture of normal thyroid tissue. It has a ground glass appearance and is brighter than muscle tissue

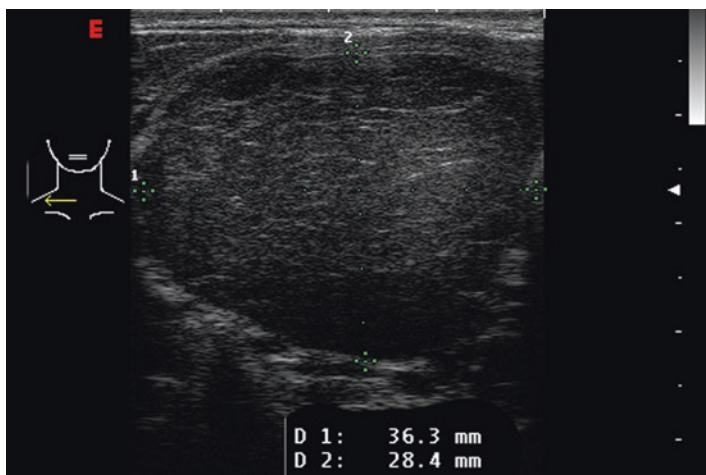


FIGURE. 2.5 The thyroid from a patient with the acutely swollen inflammatory phase of Hashimoto's thyroiditis. Massive infiltration by lymphocytes has decreased the echogenicity of the tissue resulting in a more homogeneous hypoechoic pattern



FIGURE. 2.6 A typical heterogeneous and hypoechoic pattern from Hashimoto's thyroiditis with hypoechoic inflammatory regions separated by hyperechoic fibrous tissue

## Creation of an Ultrasound Image

The earliest ultrasound imaging consisted of a sound transmitted into the body, with the reflected sound waves displayed on an oscilloscope. Referred to as A-mode ultrasound, these images in the 1960s and 1970s were capable of providing measurements of internal structures such as thyroid lobes, nodules, and cysts. Figure 2.7a shows an A-mode ultrasound image of a solid thyroid nodule. Scattered echoes are present from throughout the nodule. Figure 2.7b shows an image from a cystic nodule. The initial reflection is from the proximal wall of the cyst, with no significant signal reflected by the cyst fluid. The second reflection originates from the posterior wall. Figure 2.7c shows the A-mode image from a complex nodule with solid and cystic components. A-mode ultrasound was capable of providing size measurements in one dimension but did not provide a visual image of the structure [1].

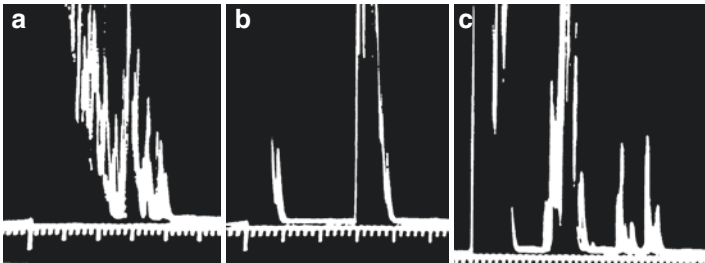


FIGURE 2.7 A-mode ultrasound images. (a) An A-mode ultrasound image of a solid thyroid nodule. Scattered echoes are present from throughout the nodule. (b) The image from a cystic nodule. The initial reflection is from the proximal wall of the cyst, with no significant signal reflected by the cyst fluid. The second reflection originates from the posterior wall. (c) The A-mode image from a complex nodule with solid and cystic components

In order to provide a visual two-dimensional image, a series of one-dimensional A-mode images are aligned as a transducer is swept across the structure being imaged. Early thyroid ultrasound images were created by slowly moving a transducer across the neck. By scanning over a structure and aligning the A-mode images, a two-dimensional image is formed. The two-dimensional image formed in this manner is referred to as a B-Mode scan (brightness mode) (Fig. 2.8). Most ultrasound transducers used for thyroid imaging use a series of piezo-electric crystals in a linear array to electronically simulate a sweep of the transducer. Firing sequentially, each crystal sends a pulse of sound wave into the tissue and receives subsequent reflections.

The final ultrasound image shows a cross sectional image through the tissue defined by the thin flat beam of sound emitted from the transducer. Resolution is the ability to distinguish between two separate, adjacent objects. For example, with a resolution of 0.2 mm, two adjacent objects measuring  $<0.2$  mm would be shown as a single object. Objects smaller

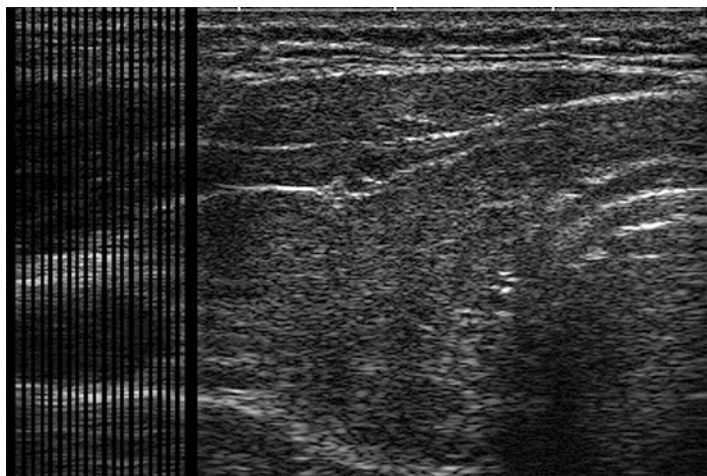


FIGURE. 2.8 A B-mode ultrasound image is composed of a series of A-mode images aligned to provide a two-dimensional image

than the resolution will not be realistically imaged. Lateral resolution refers to the ability to discriminate in a transverse, or side to side, direction. Azimuthal resolution refers to the image perpendicular to the axis of the ultrasound beam; this is inherent to the transducer and cannot be adjusted. Axial resolution is the ability to discriminate objects along the path of the ultrasound beam. Axial resolution is determined by the spatial pulse length and therefore frequency. Lateral and azimuthal resolutions are dependent on the quality and focusing of the ultrasound beam.

## The Usefulness of Artifacts in Ultrasound Imaging

A number of artifacts commonly occur in ultrasound images. Unlike most other imaging techniques, such as CT scanning, artifacts are very helpful in interpreting ultrasound images. Artifacts such as shadows behind objects or unexpected areas of brightness can provide additional understanding of the properties of the materials being imaged.

When sound waves impact on an area of extreme mismatch of acoustic impedance, such as a tissue-air interface or a calcification within soft tissue, the vast majority of the sound waves are reflected, providing a very bright signal from the object's surface and an absence of imaging beyond the structure. Figure 2.9 demonstrates *acoustic shadowing* behind a calcified nodule. Figure 2.10 illustrates a coarse calcification within the thyroid parenchyma with acoustic shadowing behind the calcification. Figure 2.11 shows the typical appearance of the trachea on an ultrasound image. Because there is virtually no transmission of sound through the air-tissue interface of the anterior wall of the trachea, no imaging of structures posterior to the trachea occurs. As explained below the reflections seen behind the trachea represent reverberation artifact.

Conversely, a cystic structure transmits sound with very little attenuation, resulting in a greater intensity of sound waves behind it, compared to adjacent structures. This

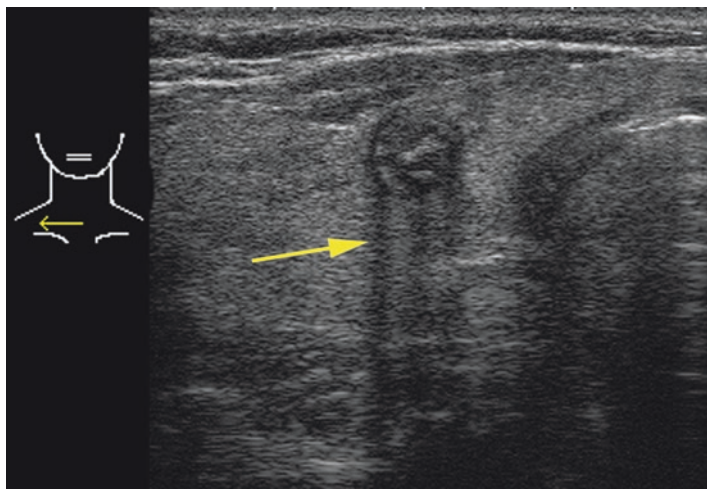


FIGURE. 2.9 Acoustic shadowing. When sound waves impact on an area of extreme mismatch of acoustic impedance, such as a calcification, the vast majority of the sound waves are reflected, resulting in the shadow beyond the structure. This calcified nodule is from a patient with familial papillary carcinoma

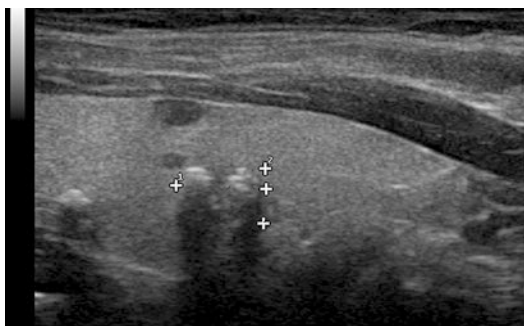


FIGURE. 2.10 Acoustic shadowing. A shadow is observed behind a coarse calcification within the thyroid parenchyma. Unlike calcification within a nodule, amorphous calcification within the parenchyma is not typically associated with malignancy

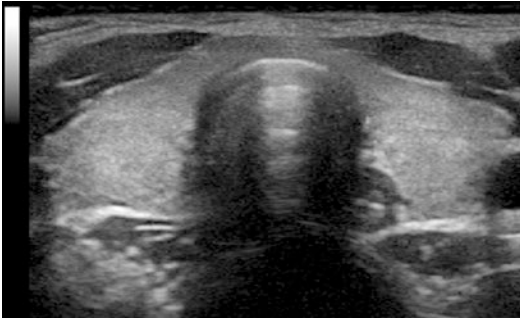


FIGURE. 2.11 Acoustic shadowing. Due to the extreme reflection from the tissue-air interface of the trachea, no image is seen behind the trachea on an anterior ultrasound

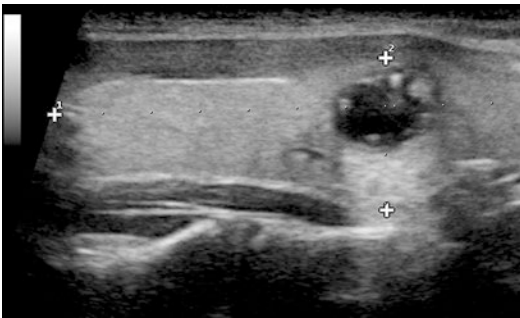


FIGURE. 2.12 Enhancement. A cystic structure transmits sound with very little attenuation, resulting in a greater intensity of sound waves behind it. Enhancement is typical behind a cystic nodule

“through transmission” results in acoustic *enhancement* with a brighter signal behind a cystic or anechoic structure. This enhancement can be used to distinguish between a cystic and solid nodule within the thyroid. Figure 2.12 illustrates enhancement behind a cystic nodule. Enhancement is not limited to cystic nodules, however. Any structure that causes minimal attenuation of the ultrasound signal will have

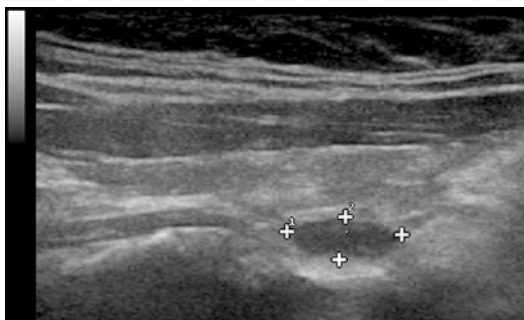


FIGURE. 2.13 Enhancement. Parathyroid adenomas have relatively homogeneous tissue and, like a parathyroid cyst, may demonstrate enhancement behind them

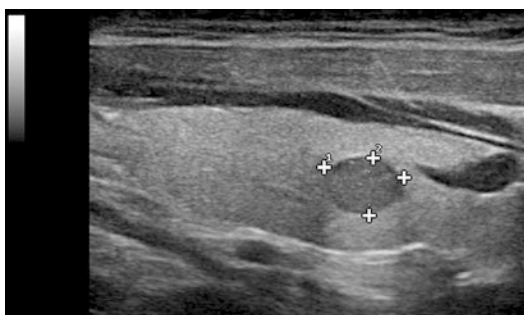


FIGURE. 2.14 Enhancement. This benign colloid nodule has a high content of fluid and colloid with a result in decrease in cellularity. The decreased attenuation of signal within the nodule results in enhancement despite it being a solid nodule

enhancement posterior to it. Figure 2.13 illustrates enhancement behind a solid parathyroid adenoma. Figure 2.14 illustrates enhancement behind a benign colloid nodule. Due to the high content of fluid and colloid within the nodule, and resultant decrease in cellularity, there is less attenuation of signal within the nodule than within the surrounding thyroid

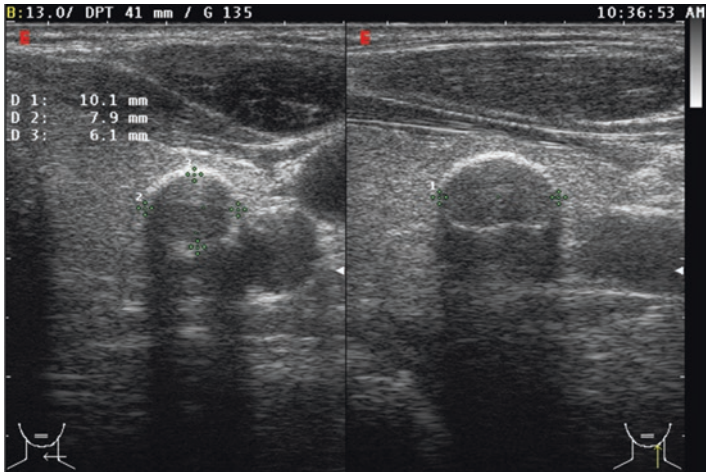


FIGURE. 2.15 Eggshell calcification. A layer of calcium surrounding the nodule results in reflection from the surface, along with marked posterior acoustic shadowing

tissue. To establish that a structure is cystic, use Doppler (as described in Chap. 3) to confirm there is no internal flow as would be seen in a vascular solid nodule with which posterior enhancement can also be seen.

Figure 2.15 shows a nodule exhibiting “eggshell” calcification. A thin layer of calcium surrounding the nodule results in an absence of reflected signal behind the nodule. As can be seen in the figure, reflection is greatest from the surfaces perpendicular to the sound waves: the front and back walls. Because the angle of incidence approaches  $180^\circ$  along the side walls, most of the reflected waves are reflected away from the transducer, resulting in a decreased signal corresponding to the sides of the structure.

*Edge artifacts* are extremely useful in identifying nodules in the thyroid. Figure 2.16 shows dark lines extending posteriorly from the sides of a nodule, aligned with the ultrasound beam. This is also an example of a reflection artifact. As

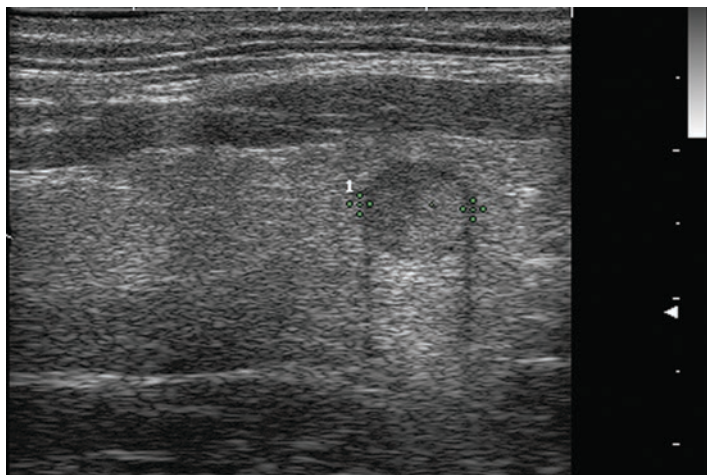


FIGURE. 2.16 Edge artifact. *Dark lines* are seen extending posteriorly from the sides of a nodule. This artifact can be used to help identify a nodule or other structure

described above, the sound waves striking the object tangentially along the sides are reflected away, rather than back toward the transducer. When two parallel dark lines are seen aligned vertically in an image, they can be followed “up” on the display to help identify a nodule or other structure.

Several artifacts arise due to reverberation. When sound waves reflect off of a very reflective surface, some may be re-reflected from the skin surface producing multiple phantom images beyond the actual image. Figure 2.17 illustrates the very common *reverberation artifact* that occurs due to this reverberation of sound waves between the skin surface and deeper tissue interfaces. Since some of the reflected sound waves will bounce back from the skin surface into the tissue multiple times, phantom images are produced. As shown, it is very common to see this artifact in the anterior aspect of cysts, raising doubt as to whether the lesion is a true cyst or partly solid. Changing the angle at which the sound strikes the lesion will usually clarify the situation. Figure 2.18 shows this common artifact behind the anterior wall of the trachea.

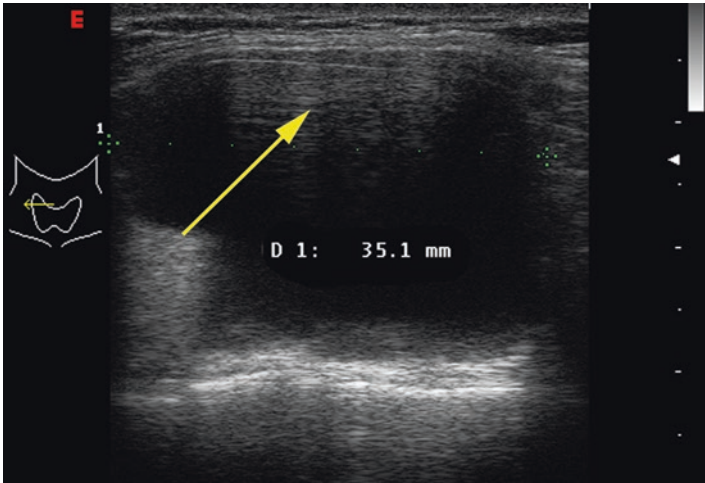


FIGURE. 2.17 Reverberation artifact. It is very common to see this artifact in the anterior aspect of cysts. This arises due to reverberation of signal between the skin surface and the anterior wall of the cyst, resulting in the late signals being received and giving the appearance of solid tissue in the anterior aspect of the cyst

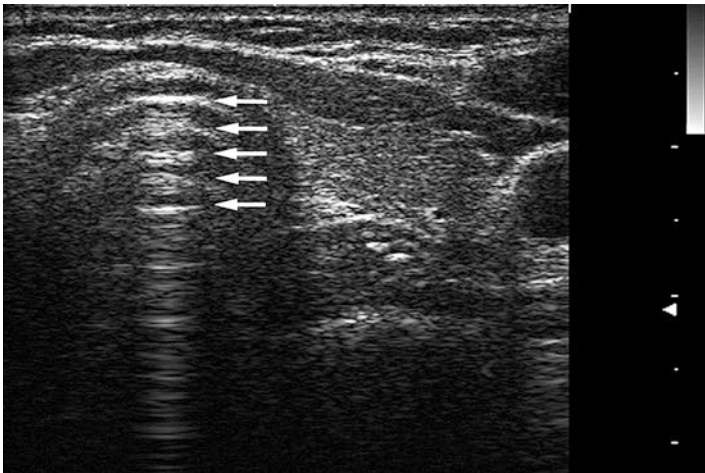


FIGURE. 2.18 Reverberation artifact. Numerous *parallel lines* are seen posterior to the anterior wall of the trachea. These may be misconstrued as tracheal rings but are actually reverberation artifact

The “comet tail” artifact is another extremely common finding arising due to reverberation [4] (Figs. 2.19, 2.20, 2.21, 2.22, and 2.23). Colloid nodules may contain tiny crystals resulting from the desiccation of the gelatinous colloid material. Reflection of the sound waves off of the crystal results in a bright spot. However, in contrast to a soft tissue calcification, the crystals begin to vibrate under the influence of the ultrasound energy. The vibration generates sound waves, which return to the transducer after the initial reflected signal, resulting in the “tail”

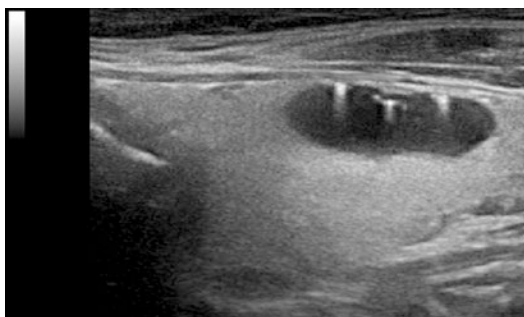


FIGURE. 2.19 “Comet tails.” Colloid nodules and cysts may contain tiny crystals resulting from the desiccation of the gelatinous colloid material. Reflection of the sound waves off of the crystal results in a bright spot. However, in contrast to a soft tissue calcification, the crystals begin to vibrate under the influence of the ultrasound energy. The vibration generates sound waves, which return to the transducer after the initial reflected signal, resulting in the “tail”

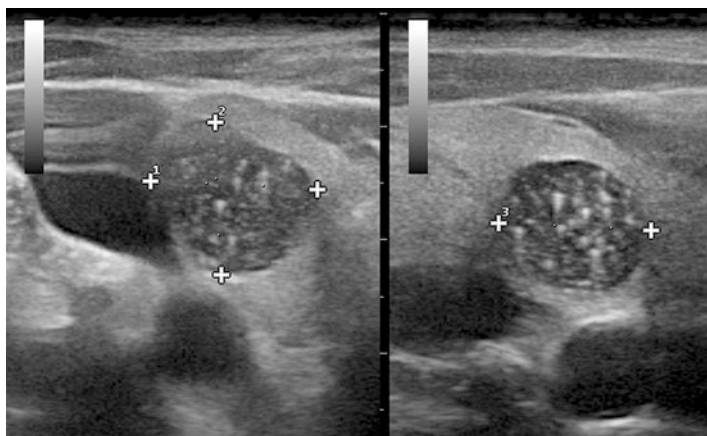


FIGURE. 2.20 “Comet tails.” Another example of comet tail artifacts within a benign spongiform nodule

tals resulting from the desiccation of the gelatinous colloid material (colloid bodies). Reflection of the sound waves off of the crystal results in a bright spot. However, in contrast to a soft tissue calcification, the suspended crystals begin to vibrate under the influence of the ultrasound energy. The vibration generates sound waves, which return to the transducer after the initial reflected signal. Also referred to as a *ring-down artifact* or *stepladder artifact*, these “comet tails” help differentiate between the typically benign densities found in a colloid nodule and highly suspicious microcalcifications. When a single comet tail is present in a small colloid cyst, it is referred to as a “cat’s eye” (Fig. 2.21). While comet tail artifacts most commonly arise within a benign colloid nodule, they may also be seen in resolving hematomas and have rarely been described within papillary carcinoma [5].

At times differentiating a comet tail density from a microcalcification may be challenging, resulting in different opinions regarding how reassuring it is to observe comet tail densities within a nodule. Tahvildari et al. assessed the characteristics of punctate echogenic reflectors in papillary carcinoma and elucidated “microcalcifications” as arising from a variety of etiologies including psammomatous calcifications, dystrophic calcifications, and eosinophilic colloid. Thus the

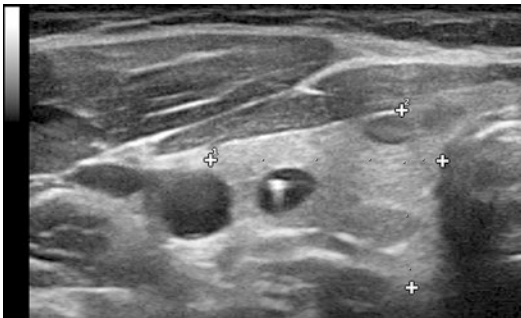


FIGURE. 2.21 “Cat’s eye” artifact. The comet tail artifact is also referred to as a ring-down artifact, a stepladder artifact, or, when a single comet tail is seen within a small colloid cyst, a cat’s eye

terms “punctate echogenic foci” or microreflectors may be more accurate terms [6]. Beland et al. suggested that non-shadowing brightly echogenic linear foci with or without a comet tail artifact may be a benign finding [5]. On the other hand, Malhi et al. concluded that all categories of echogenic foci, except those with large comet tail artifacts, are associated with cancer risk [7]. It helps in the distinction between comet tails and microcalcifications to note that comet tails typically are located either within or on the edge of a cyst, whereas microcalcifications occur within solid tissue.

Figure 2.22 illustrates a large comet tail artifact, exceeding one mm in size, in a clearly benign colloid cyst. Figure 2.23 demonstrates multiple tiny punctate echogenic reflectors in a benign hyperplastic colloid nodule. Some, but not all, have a small comet tail artifact associated. Those reflectors not showing a clear comet tail may be posterior acoustic enhancement behind the microcystic areas. In contrast, Fig. 2.24 shows typical microcalcifications within a papillary carcinoma. Visualization of these various echogenic foci is best appreciated in real-time imaging and can be enhanced by imaging at lower frequencies.

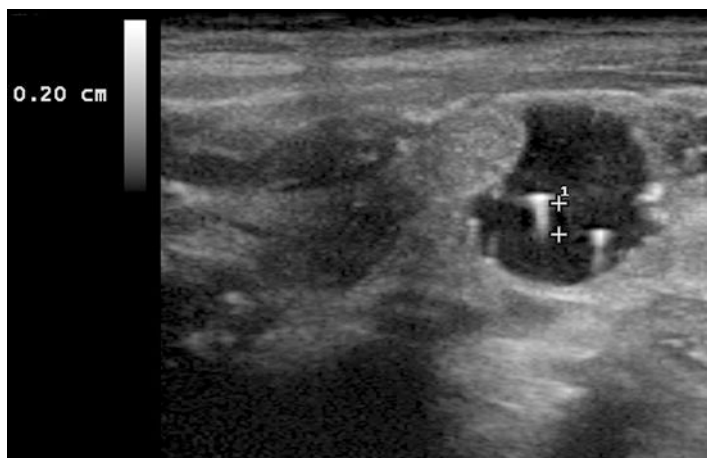


FIGURE. 2.22 A large comet tail artifact, exceeding 1 mm in size, in a benign colloid cyst

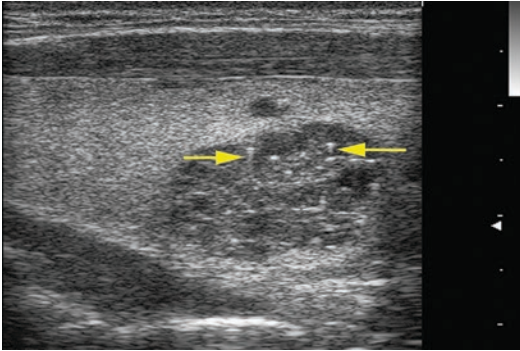


FIGURE. 2.23 Multiple comet tails and punctate echogenic foci or microreflectors within a benign spongiform nodule. Some, without tails could be mistaken for microcalcifications. Note the association with the numerous microcystic areas, behind which posterior acoustic enhancement is seen

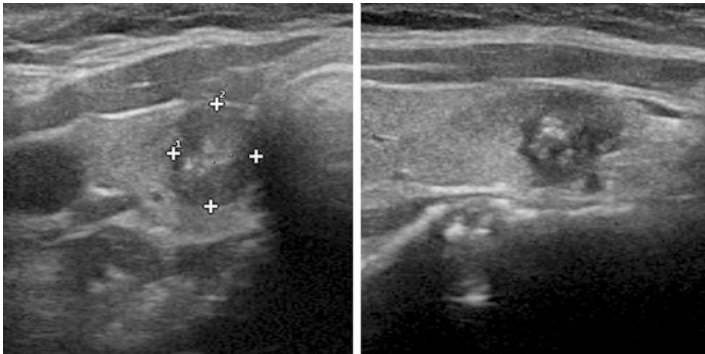


FIGURE. 2.24 Microcalcifications. Compare to the punctate echogenic foci shown in Figs. 2.20 and 2.23. Microcalcifications are typically found in solid nodules, while comet tails are seen associated with cystic or microcystic areas

Refraction is the alteration of direction of the transmitted sound at an acoustic interface when the angle of incidence is not  $90^\circ$ . A portion of a sound wave striking an interface at  $90^\circ$  is transmitted straight through. When waves strike at an angle

other than  $90^\circ$ , the transmitted wave is bent as it propagates through the interface. A greater degree of mismatch of acoustic impedance between tissues results in a greater degree of refraction. While not typically seen in near field ultrasound used in thyroid and other small parts imaging, refraction artifacts can result in a second “ghost” image when a refracting object exists in the path of an ultrasound beam.

As sound waves propagate through any tissue, the intensity of the wave is *attenuated*. Attenuation of acoustic energy results from a combination of reflection, scattering, and absorption, with conversion of sound energy to heat. Attenuation is frequency dependent, with higher frequencies having greater attenuation. As a result, while higher frequencies provide improved resolution, the depth of imaging decreases with increasing frequency. Current ultrasound technology utilizes sound waves as high as 18 MHz for thyroid imaging. However, imaging is limited to less than 5 cm of depth at this frequency. Visualization of deeper structures, as with abdominal or pelvic ultrasound, requires lower frequencies. In obese patients or when imaging very deep structures, frequencies of 5–7.5 MHz may be needed for adequate penetration and visualization of the deep neck structures. Figures 2.25 and 2.26 compare images made at 7.5 and 15 MHz. Loss of detail of proximal structures with improved imaging of deeper structures is evident with the lower frequency.

Shadowing and enhancement, as described above, are examples of attenuation artifacts. Shadowing occurs behind structures with extreme acoustic mismatch due to the attenuation of transmission of sound waves caused by nearly complete reflection. Enhancement occurs behind structures with little to no attenuation, with higher intensity sound waves present behind the structure in comparison to the adjacent tissues.

## Advances in Ultrasound Imaging

Ultrasound transducers consist of an array of crystals capable of transmitting and receiving ultrasound energy. Piezoelectric crystals vibrate when exposed to an electrical

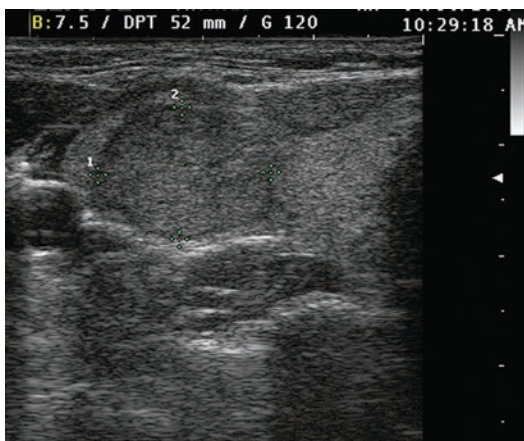


FIGURE. 2.25 Comparison of images produced with frequencies of 7.5 and 13 MHz. In this image utilizing 7.5 MHz, the nodule is less well defined, but the posterior structures are better visualized. Compare to Fig. 2.23

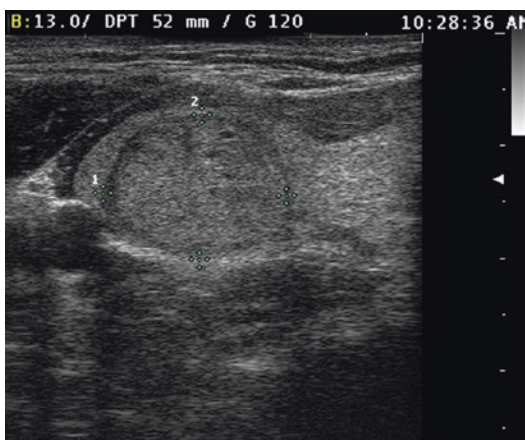


FIGURE. 2.26 Comparison of images produced with frequencies of 7.5 and 13 MHz. In this image, utilizing 13 MHz the nodule show much better definition. Compare to Fig. 2.22

current. Conversely, when energy strikes the crystal, it results in an electrical signal, with a frequency corresponding to the frequency of the incident sound wave. Thyroid ultrasound typically uses a linear array of several hundred crystals within a transducer. The transverse width of the image produced is equal to the length of the array of crystals in the transducer (often referred to as the “footprint”). Curved array (convex) transducers are less often used in thyroid ultrasound (but are commonly used in abdominal, pelvic, and cardiac imaging). By producing a divergent beam of ultrasound they allow visualization of structures larger than the transducer. Microconvex transducers are occasionally used as an aid in fine-needle aspiration biopsy, but the image produced has spatial distortion due to the lack of a linear relationship between the transverse and longitudinal planes (see Chap. 12).

Once received, the ultrasound signal undergoes image reconstruction, followed by image enhancement. Noise reduction and edge sharpening algorithms are used to clarify the image. Most ultrasound equipment allows the user to select the degree of noise reduction, dynamic range, and edge sharpening, to optimize image quality. Ultrasound equipment allows for user adjustment of the gain of the received signal. Overall gain can be adjusted, and separate channels corresponding to individual depths may be adjusted (time gain compensation) to provide the best image quality at the region of interest. Most ultrasound equipment also allows for user adjustment of the focal zone, the depth at which the ultrasound beam is optimally focused in order to improve lateral resolution. Multiple focal zones may also be selected on most ultrasound equipment. While providing an increase in the area of optimal image sharpness, the use of multiple focal zones typically slows the refresh rate of the image, resulting in a more jumpy image when visualized during real-time scanning.

While standard ultrasound receives only the frequency identical to that transmitted for imaging, tissue harmonic imaging capitalizes on the tendency of tissues to reverberate when exposed to higher power ultrasound energy. Different

tissues have a different degree of reverberation and produce unique signatures of tissue harmonics (multiples of the original frequency). Selective detection and processing of the harmonic signal produces an alternative image. Because higher frequencies are being detected, the resolution may be improved, but the original transmitted frequency is typically lower when using tissue harmonic imaging. Since the distance traveled by a harmonically generated signal is one half that of the transmitted and received signal, there is less noise. The increased resolution and decreased noise may result in increased conspicuity of some objects [8], but tissue harmonic imaging has not had widespread application in thyroid imaging.

Recently ultrasound image quality has benefitted by transition to complete digital processing. In conventional ultrasound a linear transducer transmits and receives parallel ultrasonographic waves in a single direction. With compound spatial imaging, the ultrasound beam is electronically or mechanically steered into multiple angles. Compound spatial imaging combines multiple images obtained from different angles and reconstructs them into a single image [9]. This results in much less speckle and noise and a much more realistic appearing image (Figs. 2.27 and 2.28). Artifacts are

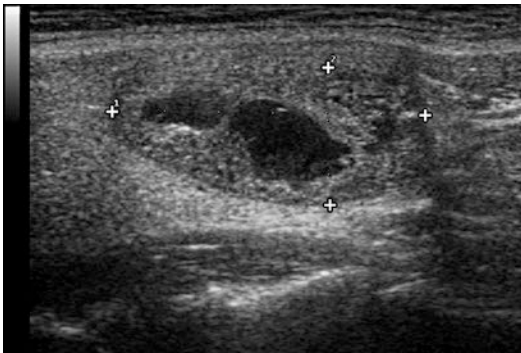


FIGURE. 2.27 A conventional ultrasound image without spatial compound imaging shows speckle artifact and more noise than the processed image shown in Fig. 2.25

reduced, but careful selection of the degree of noise reduction applied allows useful artifacts such as shadowing, enhancement, and edge artifacts to remain, aiding in interpretation of the image [10] (Figs. 2.29 and 2.30).



FIGURE. 2.28 After application of spatial compound imaging, there is a reduction of speckle artifact, less noise, and overall improved image quality

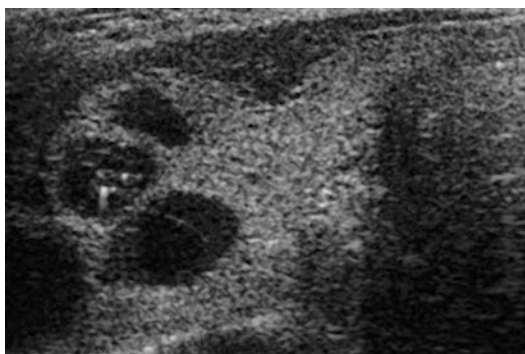


FIGURE. 2.29 A comet tail artifact and posterior acoustic enhancement are present prior to application of spatial compound imaging

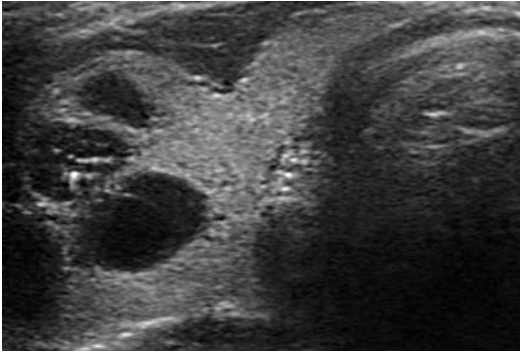


FIGURE. 2.30 The comet tail artifact and posterior enhancement remain visible with compound spatial imaging despite the reduction of speckle and noise artifact

## Quantifying Ultrasound Information

Rather than just describing a thyroid nodule as “hypoechoic and heterogeneous,” it would be preferable to describe the degree of hypoechogenicity and heterogeneity. In an effort to quantify the ultrasonographic characteristics typically used to predict malignancy, several investigators have applied mathematical analysis of the ultrasound data. Kim et al. [11] performed histogram analysis of grayscale ultrasound images and demonstrated the ability to differentiate lymphocytic thyroiditis from normal thyroid tissue. As discussed in Chap. 6, hypoechogenicity and heterogeneity are typical characteristics of thyroiditis. Histogram analysis allows for quantitation of the degree of hypoechogenicity and heterogeneity, as well as the skew and kurtosis (flatness or pointiness around the peak), providing an objective and reproducible mathematical analysis of the image. It is likely that similar assessment will be performed on thyroid nodules to assess the degree of degree of hypoechogenicity and characteristics of heterogeneity, with possible application to prediction of malignant potential. Several additional studies have begun

preliminary investigation of quantifying ultrasound characteristics of nodules. Song et al. analyzed 16 texture-based gray-level co-occurrence matrix features, providing objective quantified data with the ability to help in the prediction of malignancy of thyroid nodules [12]. Similarly, Ardakani et al. utilized wavelet texture analysis to provide a quantification of the texture of thyroid nodules, also demonstrating utility in differentiating benign from malignant nodules [13]. It is likely that in the future, mathematical quantitative analysis of ultrasound images will lead to more reproducible quantified information regarding nodules with increased power to recognize malignant features and to identify more aggressive lesions.

## Summary

In summary, ultrasound waves differ from electromechanical waves in that sound transmission is dependent on the conducting medium. Acoustic energy is reflected at interfaces of mismatch of acoustic impedance, and analysis of the reflected ultrasound waves allows construction of an image. The resolution of an ultrasound image is dependent on the frequency, the focused beam width, and the quality of the electronic processing. Resolution improves with higher frequencies, but the depth of imaging decreases. Image artifacts such as shadowing and enhancement provide useful information, rather than just interfering with creation of a clear image. The current image quality, affordable cost, and ease of performance make real-time ultrasound an integral part of the clinical evaluation of the thyroid patient.

## References

1. Meritt CRB. Physics of ultrasound. In: Rumack CM, Wilson SR, Charboneau JW, Levine D, editors. Diagnostic ultrasound. 4th ed. St. Louis: Mosby; 2011. p. 2–33.
2. Levine RA. Something old and something new: a brief history of thyroid ultrasound technology. *Endocr Pract.* 2004;10(3):227–33.

3. Coltrera MD. Ultrasound physics in a nutshell. *Otolaryngol Clin N Am*. 2010;43(6):1149–59.
4. Ahuja A, Chick W, King W, Metreweli C. Clinical significance of the comet-tail artifact in thyroid ultrasound. *J Clin Ultrasound*. 1996;24(3):129–33.
5. Beland MD, Kwon L, Delellis RA, Cronan JJ, Grant EG. Non-shadowing echogenic foci in thyroid nodules: are certain appearances enough to avoid thyroid biopsy? *J Ultrasound Med*. 2011;30(6):753–60.
6. Tahvildari AM, Pan M, Kong CS, Desser T. Sonographic pathologic correlation for punctate echogenic reflectors in papillary thyroid carcinoma. What are they? *J Ultrasound Med*. 2016;35(8):1645–52.
7. Malhi H, Beland MD, Cen SY, Allgood E, et al. Echogenic foci in thyroid nodules: significance of posterior acoustic artifacts. *Am J Roentgenol*. 2014;203(6):1310–6.
8. Szopinski KT, Wysocki M, Pajk AM, et al. Tissue harmonic imaging of thyroid nodules: initial experience. *J Ultrasound Med*. 2003;22(1):5–12.
9. Lin DC, Nazarian L, O’Kane PL, et al. Advantages of real-time spatial compound sonography of the musculoskeletal system versus conventional sonography. *Am J Roentgenol*. 2002;179(6):1629–31.
10. Shapiro RS, Simpson WL, Rauch DL, Yeh HC. Compound spatial sonography of the thyroid gland: evaluation of freedom from artifacts and of nodule conspicuity. *Am J Roentgenol*. 2001;177:1195–8.
11. Kim GR, Kim EK, Kim SJ, Ha EJ, et al. Evaluation of underlying lymphocytic thyroiditis with histogram analysis using grayscale ultrasound images. *J Ultrasound Med*. 2016;35(3):519–26.
12. Song G, Xue F, Zhang CA. Model using texture features to differentiate the nature of thyroid nodules on sonography. *J Ultrasound Med*. 2015;34(10):1753–60.
13. Ardakani AA, Gharbali A, Mohammadi A. Classification of benign and malignant thyroid nodules using wavelet texture analysis of sonograms. *J Ultrasound Med*. 2015;34(11):1983–9.

Thyroid and Parathyroid Ultrasound and  
Ultrasound-Guided FNA

Duick, D.S.; Levine, R.A.; Lupo, M.A. (Eds.)

2018, XIV, 546 p. 330 illus., 220 illus. in color.,  
Softcover

ISBN: 978-3-319-67237-3